Langmuir
Article
pubs.acs.org/Langmuir

Influence of Architecture on the Interaction of Negatively Charged Multisensitive Poly(*N*-isopropylacrylamide)-*co*-Methacrylic Acid Microgels with Oppositely Charged Polyelectrolyte: Absorption vs Adsorption

Jochen Kleinen, Andreas Klee, and Walter Richtering*

Institute of Physical Chemistry, RWTH Aachen University, Landoltweg 2, D-52056 Aachen, Germany

Received February 8, 2010. Revised Manuscript Received March 26, 2010

Two sets of core−shell microgels composed of temperature-sensitive poly(*N*-isopropylacrylamide) (PNiPAM) with different spatial distribution of pH-sensitive methacrylic acid (MAA) groups were prepared. The cores consist of either PNiPAM (neutral core; *nc*) or PNiPAM-*co*-MAA (charged core; *cc*). A charged shell existing of PNiPAM-*co*-MAA was added to the neutral core (yielding neutral core−charged shell; *nccs*), on the charged core, on the other hand, a neutral shell of PNiPAM was added (charged core−neutral shell; *ccns*). Complexes of these microgels with positively charged poly(diallyldimethylammonium chloride) (PDADMAC) of different molar masses were prepared. The amount of bound polyelectrolyte was quantified, and the microgel−polyelectrolyte complexes were characterized with respect to electrophoretic mobility and hydrodynamic radius. The penetration of polyelectrolyte into the microgel was also monitored by means of lifetime analysis of a fluorescent dye covalently bound to poly(L-lysine) providing information on the probe's local environment. The architecture of the microgel has a significant influence on the interaction with oppositely charged polyelectrolyte. Complexes with microgel with the charged shell tend to flocculate at charge ratios of 1 and are thus similar to polyelectrolyte complexes with rigid colloidal particles. Complexes with microgels that consist of a charged core and a neutral shell show very different properties: They are still temperature sensitive and reveal an influence of the polyelectrolyte's chain length. Low molecular weight PDADMAC can penetrate through the neutral shell into the charged core, and thus nearly no charge reversal occurs. The high-MW polyelectrolyte does not penetrate fully and leads to charge reversal. The results demonstrate that microgels are able to absorb or adsorb polyelectrolytes depending on the polyelectrolyte's chain length and the microgels architecture. Complexes with different surface properties and different colloidal stability can be prepared, and polyelectrolytes can be encapsulated in the microgel core. Thus, multisensitive core−shell microgels combine permeability and compartmentalization on a nanometer length scale and provide unique opportunities for applications in controlled uptake and release.

Introduction

Microgels are nanosized, cross-linked polymer particles swollen by solvent, and the degree of swelling can be controlled by the quality of the solvent. If the quality changes from good to poor, solvent is expelled from the inside of the microgel and the microgel collapses. The most often employed temperature-sensitive microgel system is poly(*N*-isopropylacrylamide), PNiPAM, which becomes insoluble in water at 32 °C; however, this volume phase transition is completely reversible.[1,2] The volume phase transition temperature (VPTT) and therefore the swelling can be adjusted via the hydrogen-bonding pattern by incorporating different comonomers[3] or by charged comonomers. In the latter case, comonomers that can be (de)protonated yield very interesting properties since these microgels are then multi (temperature and pH)-sensitive.[4−6]

The distribution of the single comonomers inside the microgel is a fundamental parameter which influences the temperature- and/or pH-induced swelling of the microgel, since charged groups located in a loosely cross-linked shell can contribute better to the swelling of a microgel as compared to charged monomers in the core of the microgel.[7] Core−shell microgels[8] can be prepared by two-step synthesis. First the core is polymerized and used as a seed in a second reaction to yield the core−shell microgel. This sequential procedure allows the spatial separation of the functional (or sensitive) monomers leading e.g. to systems with highly cross-linked shells.[9]

The interaction of microgels with charged and uncharged molecules[10] and surfactants[11−14] is widely studied since the thermoresponsive nature of the microgels offers a wide range of applications, and especially the field of drug and enzyme uptake and release is promising.[15−20] However, only few studies on

*Corresponding author. E-mail: richtering@rwth-aachen.de.

(1) Pelton, R. *Adv. Colloid Interface Sci.* **2000**, *85*, 1–33.
(2) Nayak, S.; Lyon, L. A. *Angew. Chem.* **2005**, *117*, 7862–7886.
(3) Keerl, M.; Smirnovas, V.; Winter, R.; Richtering, W. *Macromolecules* **2008**, *41*, 6830–6836.
(4) Ito, S.; Ogawa, K.; Suzuki, H.; Wang, B.; Yoshida, R.; Kokufuta, E. *Langmuir* **1999**, *15*, 4289–4294.
(5) Jones, C. D.; Lyon, A. *Macromolecules* **2000**, *33*, 8301–8306.
(6) Pich, A.; Tessier, A.; Boyko, V.; Lu, Y.; Adler, H. J. *Macromolecules* **2006**, *39*, 7701–7707.
(7) Jones, C. D.; Lyon, L. A. *Macromolecules* **2003**, *36*, 1988–1993.
(8) Sun, Q.; Deng, Y. *Langmuir* **2005**, *21*, 5812–5816.
(9) Berndt, I.; Pederson, J. S.; Richtering, W. *Angew. Chem., Int. Ed.* **2005**, *45*, 1737–1741.
(10) Hoare, T.; Pelton, R. *Langmuir* **2008**, *24*, 1005–1012.
(11) Kokufuta, E.; Zhang, Y.-Q.; Tanaka, T.; Mamada, A. *Macromolecules* **1993**, *26*, 1053–1059.
(12) Tam, K.-C.; Ragaram, S.; Pelton, R. *Langmuir* **1994**, *10*, 418–422.
(13) Nerapusri, V.; Keddie, J. L.; Vincent, B.; Bushnak, I. A. *Langmuir* **2007**, *23*, 9572–9577.
(14) Bradley, M.; Vincent, B.; Burnett, G. *Colloid Polym. Sci.* **2009**, *287*, 345–350.
(15) Kiser, P.; Wilson, G.; Needham, D. *J. Controlled Release* **2000**, *68*, 9–22.
(16) Nolan, C.; Gelbaum, L.; Lyon, A. *Biomacromolecules* **2006**, *7*, 2918–2922.
(17) De Geest, B.; Déjugnat, C.; Verhoeven, E.; Sukhorukov, G.; Jonas, A.; Plain, J.; Demeester, J.; De Smedt, S. *J. Controlled Release* **2006**, *116*, 159–169.
(18) Huo, D.; Li, Y.; Qian, Q.; Kobayashi, T. *Colloids Surf., B* **2006**, *50*, 36–42.
(19) Saunders, B.; Laajam, N.; Daly, E.; Teow, S.; Hu, X.; Stepto, R. *Adv. Colloid Interface Sci.* **2009**, *147*, 251–262.
(20) Kabanov, A. V.; Vinogradov, S. V. *Angew. Chem., Int. Ed.* **2009**, *48*, 5418–5429.

microgel interaction with polyelectrolytes[21−23] or polymers[24] have been reported though polyelectrolytes may serve as a model system for enzymes and proteins. Furthermore, the concept of layer-by-layer deposition of polyelectrolytes on microgels offers the possibility to merge the concept of polyelectrolyte hollow capsules[25,26] for drug delivery and the stimuli sensitivity of a microgel.[27,28]

Since the properties of the microgel are altered by the amount of bound material (surfactant, drugs, polymers, etc.), the bound amount needs to be quantified. Furthermore, the properties as e.g. the charge reversal induced by oppositely charged polyelectrolytes are an important factor influencing the stability of the complexes.[29,30] The stability of these water-soluble complexes depends on pH, salinity, mixing ratio, and architecture of the different polyelectrolytes.[31−35]

The spatial distribution of charges inside the microgel determines the interaction with polyelectrolytes. *Adsorption* onto the microgel would lead to a strong surface modification while *absorption* would require penetration into the microgel. Surface modification is important for layer-by-layer buildup while the penetration is important for uptake and release.[36]

In order to address this important issue, we prepared two sets of core−shell microgels with different spatial distribution of charges and studied the interaction with an oppositely charged polyelectrolyte poly(diallyldimethylammonium chloride) (PDADMAC) of different molecular weight ((i) low-MW sample with MW of 10−20 kg mol^{-1} and (ii) high-MW sample with MW 400−500 kg mol^{-1}). The properties of the core and core−shell microgels will be discussed in the first part; in a second part the interaction of the PDADMAC with the different microgels is described. The microgel−PDADMAC complexes were characterized with respect to size and electrophoretic mobility; the bound amount of PDADMAC was quantified by polyelectrolyte titration. In the third part the fluorescence lifetime of FITC-labeled poly(L-lysine) bound to the different microgels was analyzed. The fluorescent label is used as a probe to study the environment of the poly(L-lysine) and provides further information on the penetration of polyelectrolytes into microgels.

Experimental Section

Materials. *N*,*N*′-Methylenebis(acrylamide) (BIS) and potassium peroxodisulfate (KPS) were ordered from Merck. Methacrylic acid (MAA) was obtained by ABCR, and *N*-isopropylacrylamide (NiPAM) was purchased from Acros. The fluorescent label methacryloxyethyl thiocarbamoylrhodamine B (MRB) was purchased from Polysciences Inc.; sodium dodecyl sulfonate (SDS) was ordered from Sigma-Aldrich. Two different PDADMAC samples were used for adsorption experiments (i) low-MW sample with MW of 10−20 kg mol^{-1} and (ii) high-MW sample with MW 400−500 kg mol^{-1}. The low-molecular-weight PDADMAC was a gift by Katpol, Germany; the latter one and poly(styrenesulfonate) (PSS) with a molecular weight of 70−100 kg mol^{-1} were delivered by Aldrich. *o*-Tolidine was purchased from Serva Chemicals. FITC-labeled poly(L-lysine) (PLL^{FITC}) was ordered from Sigma-Aldrich and had a molecular weight of 30−70 kg mol^{-1}. Tris(hydroxymethyl)aminomethane (TRIS) was purchased by MP Biomedicals. All chemicals were used without further purification. Solutions for lifetime measurements were prepared with Lichrosolv water (Merck). All other solutions were prepared with double distilled water if not otherwise stated.

Microgel Synthesis. The microgels were synthesized by free radical polymerization in water. Water was heated to 75 °C and flushed with nitrogen for 1 h. The monomers were dissolved, and the reaction was started by KPS. The microgel particles were stabilized with SDS during the reaction. The synthesis were done in 1.5 L of water, the monomer concentration was 2 mass %, and the reaction was started with 1.5 g of KPS. Additionally, 0.1 wt % of MRB was added to the core synthesis. The ratio of core-to-shell monomer was 1:2 for both systems; SDS concentration was 1.5 mM (cmc = 8 mM).

After 6 h the solution was allowed to cool down overnight, and the solution was centrifuged in a Sorvall Discovery 90 ultracentrifuge for 45 min. Between each centrifugation the supernatant was removed and replaced by water to redisperse. After three cycles of centrifugation the solution was freeze-dried. Surfactant was used in all reactions to stabilize the microgel suspension at elevated temperature and to prevent coalescence.

The addition of the shells followed this procedure: The core microgel was dissolved in surfactant solution overnight, heated up, and purged with nitrogen. The shell monomers and KPS were diluted in degassed water. One-fourth of this solution was added to the reaction vessel. The rest of the solution was added over 2 h, and the reaction was run for 6 h.

The mass ratio of core to shell was determined by (i) comparing the masses of the monomers and the core in the synthesis and the obtained mass of the core−shell microgel, (ii) measuring the molar mass by static light scattering, and (iii) comparing the amount of methacrylic acid of the charged core and the charged core−neutral shell microgels. All methods gave similar results within 10% accuracy. For more details see Table 1.

Titration. Approximately 100 mg of the microgel was dissolved in 50 mL of water and titrated with 0.1 M NaOH at 25 °C. Conductometric titration yields the amount of methacrylic acid monomers inside the microgel.

Microgel solution was transferred to a tempered titration cell equipped with a nitrogen inlet and diluted to a volume of 50 mL. 0.1 M HCl was added until solutions pH was around 3. After allowing the solution to equilibrate for 30 min, portions of 2 μL of 0.1 M NaOH were added by a Methrohm 665 autotitrator. Conductivity and pH were recorded. The titrations were performed at 25 °C.

Static Light Scattering and Refractive Index Measurements. Static light scattering was performed on a modified Fica (632 nm; SLS-Sytemtechnik). The data were evaluated with SLS-Software Version 5.0. Scattering intensity was measured angular-dependent at 20 °C from 35° to 145° with 1° increment. The refractive index increment was measured at 20 °C with a differential refractometer DnDc-2010 (WGE Dr. Bures 620 nm) and differential refractometer Software Version 3.24 (Brookhaven Instruments).

Dynamic Light Scattering. Dynamic light scattering measurements were done on an ALV goniometer with a programmable cyrostat to control the temperature of the sample. Laser wavelength was 633 nm, and scattering angle was 60°. The samples were highly diluted to avoid multiple scattering.

(21) Greinert, N.; Richtering, W. *Colloid Polym. Sci.* **2004**, *282*, 1146–1149.
(22) Wong, J. E.; Muller, C. B.; Laschewsky, A.; Richtering, W. *J. Phys. Chem. B* **2007**, *111*, 8527–8531.
(23) Wong, J.; Diez-Pascual, A.; Richtering, W. *Macromolecules* **2009**, *42*, 1229–1238.
(24) Bradley, M.; Ramos, J.; Vincent, B. *Langmuir* **2005**, *21*, 1209–1215.
(25) Sukhorukov, G.; Donath, E.; Davis, S.; Lichtenfeld, H.; Caruso, F.; Popov, V.; Moehwald, H. *Polym. Adv. Technol.* **1998**, *9*, 759–767.
(26) Caruso, F. *Chem.—Eur. J.* **2000**, *6*, 413–419.
(27) Wong, J. E.; Richtering, W. *Curr. Opin. Colloid Interface Sci.* **2008**, *13*, 403–412.
(28) Möhwald, H. *Colloid Polym. Sci.* **2010**, *288*, 123–131.
(29) Bungenberg de Jong, H. G.; Kruyt, H. R. *Proc. Acad. Sci. Amsterdam* **1929**, *32*, 849.
(30) Cohen Stuart, M. A. *Colloid Polym. Sci.* **2008**, *286*, 855–864.
(31) Kabanov, A. V.; Bronich, T. K.; Kabanov, V. A.; Yu, K.; Eisenberg, A. *Macromolecules* **1996**, *29*, 6797–6802.
(32) Harada, A.; Kataoka, K. *Macromolecules* **1998**, *31*, 288–294.
(33) Cohen Stuart, M. A.; Besseling, N. A. M.; Fokkink, R. G. *Langmuir* **1998**, *14*, 6846–6849.
(34) Maarten Biesheuvel, P.; Lindhoud, S.; Cohen Stuart, M. A.; de Vries, R. *Phys. Rev. E* **2006**, *73*, 041408−1–9.
(35) Hofs, B.; de Keizer, A.; Cohen Stuart, M. A. *J. Phys. Chem. B* **2007**, *111*, 5621–5627.
(36) Bysell, H.; Malsten, M. *Langmuir* **2006**, *22*, 5476–5484.

Table 1. Properties of the Microgels[a]

	monomer feed in synthesis			titration analysis		
	NiPAM [mass %]	BIS [mass %]	MAA [mass %]	MAA [mass %]	d*n*/d*c* [mL/g]	M_w [10^8 g mol^{-1}]
neutral core *nc*	96.1	3.9			0.1891	2.1
charged shell *nccs*	90.9	3.9	5.1	3.8	0.1915	2.1
charged core *cc*	90.9	4.0	5.1	6.1	0.2275	5.1
neutral shell *ccns*	96.1	3.9		3.5	0.2299	3.6

[a] The amount of methacrylic acid in the microgel is listed in column "titration".

The samples were measured at different angles at room temperature prior to temperature-dependent runs. Samples were measured for 210 s. The reproducibility of this method is 5% or better. Error bars with 5% deviation are given for the first and last data point of temperature- and pH-dependent measurements, respectively.

Electrophoretic Mobility. Measurements of the electrophoretic mobility were performed on a NanoZS zetasizer (Malvern). The values of the electrophoretic mobility were not converted to a zeta-potential. The usual hard-sphere model may not be used to convert the mobility to a zeta-potential, since the microgels are porous, soft, and swollen by the solvent.[37] The standard deviation of the measurements was better than 10%. For the sake of clarity, error bars are given in the plots for few data points only.

Polyelectrolyte Titration. The indication of a 1:1 complex between polycation and polyanion by a dye responding to an excess of one polyion was first described 1952.[38] We use a phototitrator which was a gift by BASF and described by Horn.[39] A PSS solution was added by an autotitrator to a sample of PDADMAC which was diluted with ~100 mL of water. 20 μL of a 2 mM *o*-tolidine solution was added as indicator. Every PDADMAC solution was titrated at least three times to evaluate the concentration. The concentration of the PDADMAC stock solutions was estimated by polyelectrolyte and argentometric titration: $AgNO_3$ solution of known concentration was added to determine the concentration of the chloride counterions of the polycation.

Adsorption Experiments. Solutions of PDADMAC and microgels were mixed; water was added to give a total volume of 10 mL. After 3 days the mixture was centrifuged for 30 min at 50 000 rpm in a Sorvall Discorery 90SE. The supernatant was removed carefully and kept for further experiments. 5 mL of water was added to the precipitate in the centrifugation tube to redisperse the microgel−polyelectrolyte complex. After 2 days the redispersed complex was investigated by different techniques. Prior to use, samples of all polyelectrolyte solutions were centrifuged at 50 000 rpm for 30 min. No precipitate was formed, and the supernatant had the same polyelectrolyte concentration as the starting solution.

Mixtures of TRIS and HCL were prepared to obtain solutions with different pH values. The buffer concentration was 5 mM, and the ionic strength was adjusted to 50 mM by adding NaCl. First, the microgel was added to the solution, and then the poly(L-lysine) was added after 10−15 min. The final polyelectrolyte concentration was around 2.5×10^{-6} mass %. The ratio between microgel and polyelectrolyte was calculated by the ratio of acid (MAA) and basic (amino) groups. MAA groups were always in an excess (1.5−10 times). No lifetime dependence on the microgel/PLL ratio was observed in this range. The complete sample was allowed to equilibrate overnight before measuring.

Lifetime Measurements. A confocal microscope (PicoQuant) was used for measuring the FITC lifetime as described elsewhere.[40,41] A pulsed laser (pulse rate: 20 MHz) with an excitation wavelength of 470 nm was used. The measurements were performed at room temperature. The pH of the sample was measured (Metrohm 744 pH meter) after the measurement. The data were treated in the following standard procedure: First the background was subtracted, and the data were normalized to unity to evaluate the lifetime decay data. For each lifetime decay the data were fitted with Origin (OriginLab Corp., Version 7.5) nonlinear least-squares fitting tool. Different fitting models (multiexponentials, stretched exponential) have been tested. Best residuals were obtained with a triexponential fit:

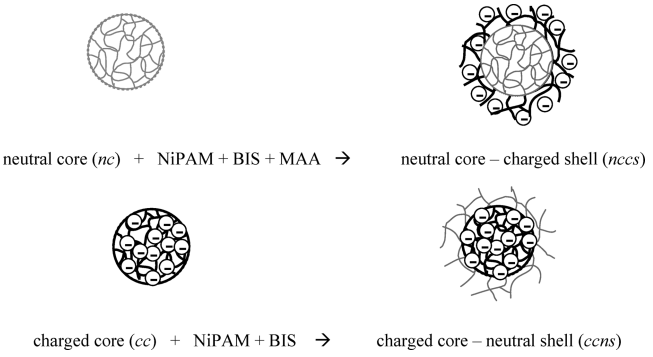

Figure 1. Schematic picture of the formation of the different core and core−shell microgels. The neutral parts of the microgels are represented by a gray network, and charged regions are shown as dark network. Microgel and mesh size are not to scale (for detailed information on the structure of microgels see refs 43 and 44).

$$F(t) = \sum_{i=1}^{3} \alpha_i \exp(-t/\tau_i)$$

with the time-dependent fluorescence intensity $F(t)$ and the amplitude α_i and the decay time τ_i for each summand i. The mean lifetime $\langle\tau\rangle$ was calculated with the equation[42]

$$\langle\tau\rangle = \frac{\sum_{i=1}^{3} \alpha_i \tau_i^2}{\sum_{i=1}^{3} \alpha_i \tau_i}$$

Results

Characterization of Core−Shell Microgels. The microgels were synthesized by sequential polymerization of first the core and after cleaning a shell was added (compare Figure 1). Core and shell consist either of cross-linked poly(NiPAM) (neutral) or cross-linked poly(NiPAM-*co*-MAA) (charged).

Adding a shell leads to a shell restricted swelling of the core.[45] The shell is added onto the collapsed core since the reaction

(37) Ohshima, H. *Colloid Polym. Sci.* **2007**, *285*, 1411–1421.
(38) Terayama, H., J. *Polym. Sci.* **1952**, *8*, 243–253.
(39) Horn, D.; Heuck, C. *J. Biol. Chem.* **1983**, *1258*, 1665–1670.
(40) Müller, C. B.; Weiss, K.; Richtering, W.; Loman, A.; Enderlein, J. *Opt. Express* **2008**, *16*, 4322–4329.
(41) Müller, C. B.; Richtering, W. *Colloid Polym. Sci.* **2008**, *286*, 1215–1222.
(42) Lacowicz, J. R. *Principles of Fluorescence Spectroscopy*, 3rd ed.; Springer: New York, 2006.
(43) Berndt, I.; Pedersen, J. S.; Richtering, W. *J. Am. Chem. Soc.* **2005**, *127*, 9372–9373.
(44) Stieger, M.; Richtering, W.; Pederson, J. S.; Lindner, P. *J. Chem. Phys.* **2006**, *120*, 6197–6206.
(45) Gan, D.; Lyon, A. *J. Am. Chem. Soc.* **2001**, *123*, 8203–8209.

Table 2. Properties of the Microgels[a]

	titration analysis	R_h [nm]		electrophoretic mobility [10^{-8} m^2 V^{-1} s^{-1}]	
	MAA [mass %]	pH 4	pH 9	pH 4	pH 9
neutral core, *nc*		130	132	−0.16	−0.13
neutral core−charged shell, *nccs*	3.8	171	320	−0.23	−1.42
charged core, *cc*	6.1	167	190	−0.18	−1.11
charged core−neutral shell, *ccns*	3.5	236	245	−0.15	−0.21

[a] The amount of methacrylic acid (in mass %) in the entire microgel and their hydrodynamic radii and electrophoretic mobilities at 20 °C and at pH = 4 and pH = 9 (see also Figure 2).

Table 3. Hydrodynamic Radii of the Core and Core−Shell Microgels at 20 and 50 °C at pH = 4[a]

	R_h [nm]		shell thickness [nm]	
	20 °C	50 °C	minimal	maximal
neutral core, *nc*	141	61	29	109
neutral core−charged shell, *nccs*	170	68		
charged core, *cc*	167	81	73	159
charged core−neutral shell, *ccns*	240	121		

[a] Comparing the core size in the swollen and collapsed size with the swollen core−shell microgel gives the minimal and maximal shell thickness.

temperature is above the VPTT. The estimation of the thickness of the shell is not trivial since the core is not rigid in contrast to other core−shell systems.[46,47] The radii of the cores and the core−shell microgels can be measured in the swollen (20 °C) and in the collapsed state (50 °C), and the shell thickness can be roughly estimated by comparing the size of the cores in the swollen and collapsed state with the size of the swollen core−shell microgel. The sizes of the cores and the core−shell microgels are listed in Table 3. The sizes were measured at pH = 4 to compare the microgels in their uncharged states. The minimal thickness of the shell is the difference of the radii at 20 °C of the core and the core−shell microgels. This thickness would be expected if the core is rigid. Full compression of the core would lead to a maximal shell thicknesses; thus, the maximal shell thickness is the difference of the collapsed cores and the swollen core−shell microgels.

In both core−shell microgels, the shells have a similar mass as the corresponding cores. The absolute masses of the microgels were determined by static light scattering (compare Table 1), providing mass ratios of core to shell of 1:1 for the *nccs* system and of 5.1/3.6 ≈ 1.4 for the *ccns* microgel. The mass balance of the synthesis as well as titration of MAA provided similar mass ratios.

The neutral core shows of course no pH dependence, whereas the charged core does. However, the pH-induced swelling is reduced by adding a neutral shell around the charged core (Figure 2). While the charged core swells by ca. 20 nm, the core−shell microgel swells less than 10 nm.

The pH-dependent measurements of the electrophoretic mobilities show the expected behavior. While the neutral core shows no pH dependence, adding the charged shell changes the behavior completely, and the core−shell microgel shows very strong pH dependence. The electrophoretic mobility of the charged core changes pH dependently, which, however, is not as pronounced as for the neutral core−charged shell microgel, since the MAA groups are not as close to the surface. Adding a neutral shell onto the charged core yields a microgel with an electrophoretic mobility which is not pH-dependent anymore, although it still contains 3.5 wt % MAA that are fully deprotonated at pH = 9.

The influence of the shell on the microgel behavior is also obvious from temperature-dependent hydrodynamic radii at pH = 9 shown in Figure 3.

The neutral core shows normal temperature-sensitive behavior; it collapses around 32 °C. By adding the charged shell, the microgel becomes much bigger and the temperature sensitivity is smeared out; thus, the charged shell prevents the microgel from full collapse.[48] The charged core behaves similar to the neutral shell−charged core microgel; its temperature sensitivity is also rather weak. However, by adding the neutral shell, the influence of charges becomes weaker and the temperature-dependent hydrodynamic radius reveals a similar trend as the neutral core, although the amount of MAA inside the microgel is similar to the neutral core−charged shell microgel.

In conclusion, the sequential synthesis of core−shell microgels lead to three charged microgels (namely charged core, *cc*; charged core−neutral shell, *ccns*; neutral core−charged shell, *nccs*), the properties of which are influenced by the architecture. The charged groups within the microgels are located either in the inside of the microgels (charged core−neutral shell) or exposed (neutral core−charged shell). Therefore, their interaction with oppositely charged polyelectrolytes is expected to be different and might also depend on the polyelectrolyte's chain length.

Interaction of PDADMAC with Core−Shell Microgels. Two PDADMAC samples with different molecular weight were used to study the interaction with the different microgels. These PDADMAC are (i) a low-MW sample with MW of 10−20 kg mol^{-1} and (ii) a high-MW sample with MW 400−500 kg mol^{-1} and were already used previously.[49] The amount of negative charges of the microgels at a certain concentration is known from titrations. Furthermore, polyelectrolyte and argentometric titration enable us to determine the concentration of PDADMAC solutions. The ratio between positive charges from the PDADMAC and the negative charges of the microgel is named initial charge ratio, *icr*.

Adding a certain amount of PDADMAC to a microgel does not necessarily lead to full binding of PDADMAC, so the true composition of the microgel−polyelectrolyte complex can vary from the *icr*. The solution containing the mixture of microgel and PDAMAC was centrifuged; the complex forms a redispersible precipitation while not attached PDADMAC stays in the supernatant and was separated. The amount of PDADMAC in the supernatant was quantified and thus allows calculating the amount of PDADMAC bound to the microgel. In the following, the composition of the complexes will be characterized by the nominal charge ratio, *ncr*. The *ncr* cannot be bigger than the *icr*. If the *ncr* = *icr*, all PDADMAC is bound to the microgel. The use of *icr* and *ncr* allows comparing the binding of different microgels with polyelectrolytes.

In Figure 4, the bound amount of low- and high-MW PDADMAC is shown for the different microgels. The left-hand

(46) Senff, H.; Richtering, W.; Norhausen, C.; Weiss, A.; Ballauf, M. *Langmuir* **1999**, *15*, 102–106.
(47) Ballauff, M.; Lu, Y. *Polymer* **2007**, *48*, 1815–1823.
(48) Jones, C. D.; Lyon, L. A. *Langmuir* **2003**, *19*, 4544–4547.
(49) Kleinen, J.; Richtering, W. *Macromolecules* **2008**, *41*, 1785–1790.

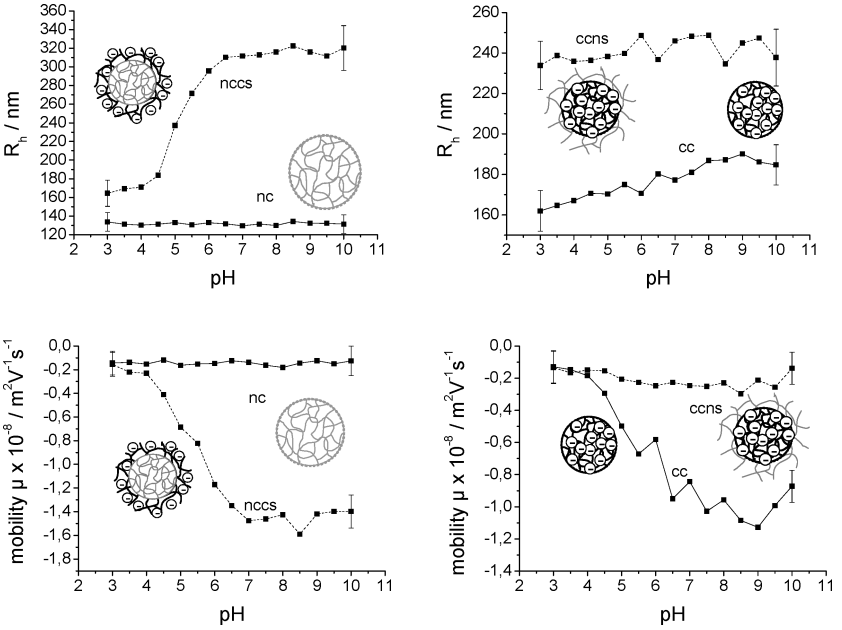

Figure 2. pH-dependent properties of the microgels. Left-hand side always shows the properties of the neutral core and neutral core−charged shell microgels; right-hand side shows properties of the charged core and charged core−neutral shell microgels. Top: hydrodynamic radii; bottom: electrophoretic mobilities. Please note that the scale of the abscissa is always the same but differs for the ordinate. Lines are guides for the eye. Measurements were performed at 20 °C.

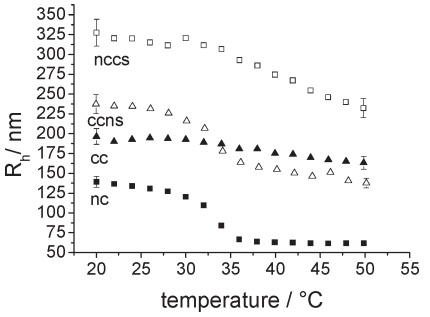

Figure 3. Temperature-dependent size of the different microgels at pH = 9 (fully deprotonated). Only heating curves are shown; cooling curves match with the heating curves.

side shows the *nccs* microgel; on the right-hand side the *cc* microgel and *ccns* microgel are shown.

The neutral core−charged shell microgel is able to bind similar quantities of low- and high-MW PDADMAC. All offered PDADMAC is bound to the microgel if $icr < 1$, but the binding is no longer quantitative if more PDADMAC is offered to the microgel. The amount of bound PDADMAC reaches a plateau at $ncr \approx 2$; thus, the complexes contain twice the amount of positive charges (PDADMAC) compared to negative charges (MAA in microgel).

In contrast, the charged core microgel and charged core−neutral shell microgel show different binding for the two PDADMAC samples. The high-MW PDADMAC binds quantitatively at $icr \leq 1.4$, and then a plateau is reached. For the low-MW PDADMAC, however, the *ncr* equals the *icr* up to a value of two. If even more low-MW PDADMAC is offered to both the *cc* and the *ccns* microgel, the binding is not quantitative anymore but a plateau is not reached.

The composition at which a plateau is reached is expected to depend on the sequence of the charged monomers in the microgel. The charge density of the microgels is lower as compared to the charge density of PDADMAC. The higher the mismatch of both charge densities, the more PDADMAC has to bind to the microgel before all negative charges can be complexed. However, the difference of the two PDADMAC samples in the binding behavior to the *cc* and *ccns* must have a different origin and will be discussed further in the Discussion. A detailed investigation of the influence of microgel charge density is beyond the scope of this publication and will be discussed in a forthcoming publication.

The electrophoretic mobilities of the obtained complexes at pH = 9 shown in Figure 5 reveal a similar behavior as the *ncr*/*icr* graphs. The molar mass of PDADMAC has no influence on the electrophoretic mobilities of the complexes with the *nccs* microgel. Only the *ncr* influences the electrophoretic mobility, and charge reversal is obtained at $ncr \approx 1$.

On the other hand, the charged core microgel and the charged core−neutral shell microgel show a dependence on the molar mass of PDADMAC. The electrophoretic mobilities of the complexes made of these microgels and high-MW PDADMAC stay at constant negative values for $ncr < 1$. Charge reversal is found at $ncr \approx 1$, and the value of the electrophoretic mobilities rise to values of $+5.0 \times 10^{-8}$ m^2 V^{-1} s^{-1}. The low-MW PDADMAC, however, shows different behavior. The electrophoretic mobility of the charged core microgel changes from negative to positive at $ncr \approx 1.6$ and reaches a constant value of around $+1.1 \times 10^{-8}$ m^2 V^{-1} s^{-1}. The electrophoretic mobilities of the complexes made of low-MW PDADMAC and the charged core−neutral shell microgel stay negative even if the number of positive charges exceeds the negative ones by a factor of 5.

In addition, the electrophoretic mobility of complexes was measured as a function of pH in order to study the influence of the degree of protonation of methacrylic acid sites on the isoelectric point (IEP).[50] In Figure 6 the electrophoretic mobilities of the complexes made of *cc* microgel and low-MW PDADMAC and of *ccns* microgel and low-MW PDADMAC are shown for pH = 3 (open symbols) and pH = 9 (filled symbols). The electrophoretic mobilities of the complexes at pH = 3 are all positive and with

(50) Schwarz, S.; Buchhammer, H. M.; Lunkwitz, K.; Jacobasch, H. J. *Colloids Surf., A* **1998**, *140*, 377–384.

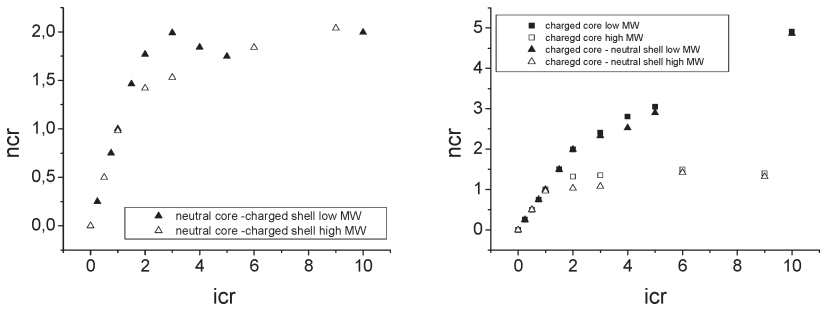

Figure 4. Composition of the complexes made of low- and high-MW PDAMAC and different microgels. The microgels were fully deprotonated (pH = 9). Filled symbols show the low-MW PDADMAC, and open symbols show the high-MW PDADMAC. The complexes prepared from *nccs* microgel are shown on the left; the complexes prepared from the charged core and the *ccns* microgels are shown on the right side.

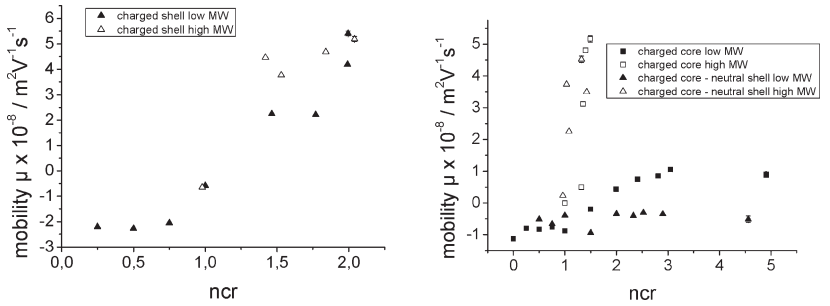

Figure 5. Electrophoretic mobilities of the complexes made of low- and high-MW PDAMAC and different microgels at pH = 9.

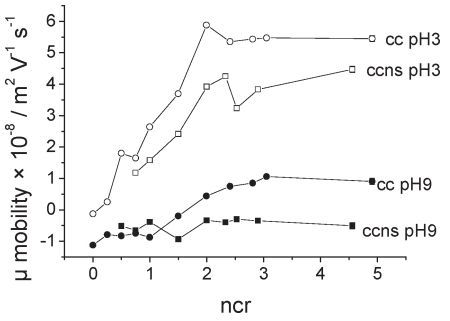

Figure 6. Electrophoretic mobility of the complexes consisting of charged core (*cc*) microgel (circles) and charged core−neutral shell (*ccns*) microgel (squares) and low-MW PDADMAC at pH = 9 (filled symbols) and pH = 3 (open symbols).

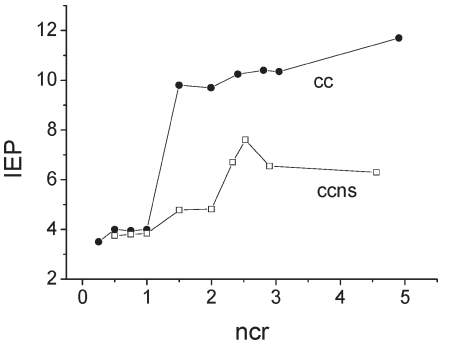

Figure 7. Isoelectric points of complexes of the charged core (*cc*) and charged core−neutral shell (*ccns*) microgels with low-MW PDADMAC as a function of composition. Filled symbols show the complexes containing the *cc* microgel, and open symbols show the *ccns* microgel.

increasing *ncr* (i.e., bound amount of PDADMAC) the electrophoretic mobility rises. At *ncr* ≥ 2 the electrophoretic mobilities of the complexes stay constant at values of $+5.7 \times 10^{-8}$ m^2 V^{-1} s^{-1} (*cc* microgel) and $+4.3 \times 10^{-8}$ m^2 V^{-1} s^{-1} (*ccns* microgel). The more PDADMAC is bound to the microgel (the higher the *ncr*), the more the isoelectric point (IEP) is shifted to basic pH. In Figure 7 the IEPs of the complexes made of the *cc* microgel and the *ccns* microgel with low-MW PDADMAC are plotted vs *ncr*. The IEPs of both investigated microgels stay around 4 for *ncr* ≤ 1. For *ncr* > 1, IEPs rise to 10 and 6 for the *cc* and *ccns* microgel, respectively. When the pH was changed back to pH = 9, the same values for the electrophoretic mobility were obtained. Obviously, the microgel−polyelectrolyte complexes with the low-MW PDADMAC are very stable. Also, temperature-dependent size measurements showed normal behavior of the complexes of *cc* and *ccns* microgel and low-MW PDADMAC (see Supporting Information, Figures S1 and S2). The complexes of *nccs* microgel and PDADMAC showed no temperature sensitivity, indicating the formation of a physically cross-linked shell (see Supporting Information, Figure S3).

The complexes with the high-MW PDADMAC showed either flocculation or the complexes gave not the same electrophoretic mobilities when the pH was changed from pH = 9 to acidic and back to basic conditions. The hydrodynamic radii of the complexes at 20 °C of the complexes with high MW PDADMAC are shown in the Supporting Information (Figure S4).

Apparently, complexes with the high-MW PDADMAC are not as stable as complexes with the low-MW PDADMAC when the pH is changed after preparation. This is contrary to normal polyelectrolyte complexes since usually higher number of binding sites for high-MW polyelectrolyte enhanced complex stability. The behavior can be explained with the different penetration of the two PDADMAC samples. The low-MW PDADMAC can penetrate into the microgels and can form multiple binding sites

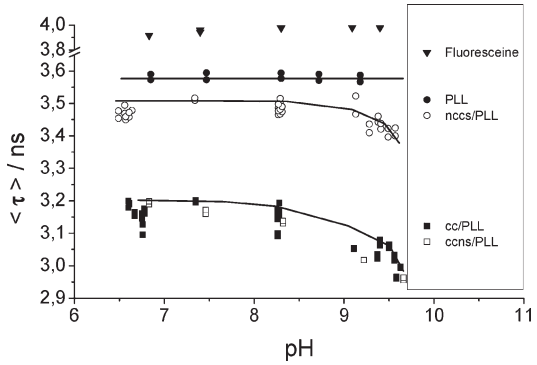

Figure 8. Plot of the pH dependence of the mean lifetime for complexes between PLL^{FITC} and different microgels. The lines are guides to the eyes.

with MAA groups. The penetration of the high-MW PDADMAC is, however, hindered, and less binding sites are formed.

Lifetime Measurements: Interaction of PLL with Core−Shell Microgels. The lifetime of fluorescent dyes can depend on the dye's local environment, and thus lifetime data can provide interesting information on the interpenetration of polyelectrolytes and microgels.[42] The pH-dependent lifetime of free fluoresceine and of PLL^{FITC} is displayed in Figure 8. Free fluoresceine shows a lifetime around 4 ns comparable to values in the literature[51] and is nearly pH-independent for the investigated pH range. PLL^{FITC} shows a slightly lower lifetime of around 3.5−3.6 ns, but the lifetime is still independent of pH. The lifetime is also independent of the PLL concentration.

Figure 8 shows as well the lifetime vs pH for complexes formed by PLL^{FITC} and different microgels. Comparing the different microgel/PLL systems, two groups are found. On the one hand, the complexes formed by *cc* and *ccns* (with *cc* as core) show nearly the same behavior. Starting with a lifetime around 3.15 ns at pH = 6.5, the lifetime decreases at higher pH. On the other hand, *nccs*, the microgel with the charge in the shell, reveals a lifetime around 3.45 ns at pH = 6.5, which is in between free PLL and the complexes with *cc* and *ccns* microgels. The pH dependence is similar for all complexes.

The data in Figure 8 show that different lifetimes were observed for different groups of samples. The lifetime of the FITC-labeled PLL shows no pH dependence just as free fluoresceine, indicating that PLL has the same chain conformation in the investigated pH range. PLL adopts a random coil conformation under these conditions; denser conformations like α-helix or *β*-sheet where dye label and PLL chain have more possibilities to get in contact are stable only at higher ionic strengths or pH values.[52−56]

The complexes of PLL^{FITC} with the *nccs* microgel reveal a lifetime in between free PLL and the complexes with for the *cc* and *ccns* microgels. The polyelectrolyte will be located in the charged shell of the *nccs* microgel as the polymer−microgel interaction is dominated by electrostatics. The relatively high lifetime, which is close to the value for free PLL, indicates that the shell provides an environment for the PLL which is similar to that of free PLL. This is in good agreement with the low segment density of such microgels at the surface as compared to the interior and indicates that PLL is located at the surface of the *nccs* microgel.

Discussion

Three different microgels were prepared with distinctly different spatial distribution of MAA groups, which leads to distinctly different sensitivity of size and electrophoretic mobilitiy to temperature and pH. These microgels are used as model systems to study the interaction with oppositely charged polyelectrolytes.

First we discuss the interaction of the different microgels with PDADMAC.

***nccs* Microgel.** In Figure 4 on the left side the *icr*/*ncr* graph for the *nccs* microgel is shown. Both MW PDADMAC interact in similar quantities, and also the measurements of the electrophoretic mobility (Figure 5, left) yield similar results. The charged moieties of this microgel are located in the loosely cross-linked shell and are thus easily accessible for the polyelectrolyte and PDADMAC penetrates into this shell independent of chain length. The complex made of high-MW PDADMAC with *ncr* = 1 is not stable (data not shown) but forms aggregates. Increased binding of PDADMAC leads to a stabilization, as e.g. monitored by the electrophoretic mobility (Figure 5). The behavior of the *nccs* microgel is similar to rigid colloidal particles. Complexes of e.g. latex particles and oppositely charged polyelectrolytes tend to flocculate at charge ratios of 1.[57−59] In addition, quantitative studies revealed also no influence of the polyelectrolyte's chain length.[60] Obviously, the different surface structure of a microgel as compared to a rigid particle does not significantly alter polyelectrolyte binding when the microgel charges are located near the surface.

***cc* and *ccns* Microgels.** These microgels bind less of the high-MW than of the low-MW-PDADMAC. This indicates that the high-MW PDADMAC is less able to penetrate into the microgel as compared to the shorter polyelectrolyte. Comparing the amounts of PDADMAC bound to the *cc* and *ccns* microgels reveals that the binding is exclusively driven by electrostatics. A significant unspecific binding would lead to a different development of the composition of the complexes, and more PDADMAC would bind to the *ccns* microgel as compared to the *cc* microgel. The addition of the uncharged shell onto the charged core, however, did not lead to additional binding of PDADMAC.

The electrophoretic mobilities of the complexes containing high-MW PDADMAC turn from negative to positive at *ncr* = 1 and rise to high values. The electrophoretic mobilities of complexes containing low-MW PDADMAC, however, turn hardly positive (*cc* microgel) or remain negative (*ccns* microgel).

These results indicate that both polyelectrolytes are able to penetrate through the noncharged shell, however, to a different extent. Apparently, the low-MW sample penetrates to the charged core, and thus nearly no charge reversal occurs. The high-MW polyelectrolyte does not penetrate fully and leads to charge reversal. This behavior is schematically illustrated in Figure 9.

This different degree of penetration also explains the different colloidal stability of the complexes. The low-MW PDADMAC is bound inside the core, and thus the complexes are stabilized by the neutral shell preventing aggregation. Complexes with the high-MW PDADMAC have polycation chains at the surface, leading to a positive electrophoretic mobility. These chains can also lead to aggregation via bridging or patches and thus explain the reduced stability as compared to complexes with low-MW PDADMAC.

(51) Sjöback, R.; Nygren, J.; Kubista, M. *Spectrochim. Acta, Part A* **1995**, *51*, L7–L21.
(52) Townend, R.; Kumosinski, T. F.; Timashe, S. N.; Fasman, G. D.; Davidson, B. *Biochem. Biophys. Res. Commun.* **1966**, *23*, 163–169.
(53) Greenfield, N.; Fasman, G. D. *Biochemistry* **1969**, *8*, 4108–4116.
(54) Painter, P. C.; Koenig, J. L. *Biopolymers* **1976**, *15*, 229–240.
(55) Yasui, S. C.; Keiderling, T. A. *J. Am. Chem. Soc.* **1986**, *108*, 5576–5581.
(56) Sjögren, H.; Ulvenlund, S. *Biophys. Chem.* **2005**, *166*, 11–21.
(57) Bauer, D.; Killmann, E.; Jaeger, W. *Colloid Polym. Sci.* **1998**, *276*, 698–708.
(58) Rehmet, R.; Killmann, E. *Colloids Surf., A* **1999**, *149*, 323–328.
(59) Buchhammer, H.-M.; Petzold, G.; Lunkwitz, K. *Langmuir* **1999**, *15*, 4306–4310.
(60) Rehmet, R.; Killmann, E. *Colloids Surf., A* **1999**, *149*, 323–328.

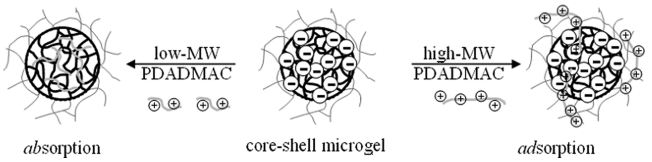

Figure 9. Schematic illustration of the binding of low- and high-MW PDADMAC to the charged core−neutral shell microgel. The low-MW PDADMAC can penetrate through the shell and the electrophoretic mobility of the complexes stay negative (left side). The high-MW PDADMAC adsorbs to the surface of the microgel, leading to a strong surface modification and charge reversal (right side).

The *ccns* microgel can be compared with porous materials as fibers,[61,62] microspheres,[63] porous glass,[64] or columns for chromatography.[65,66] The binding of PDADMAC to these materials depends on the molecular weight of the polycation. The studies further revealed that low-molecular-weight polyelectrolyte binds to a bigger extend as compared to high-molecular-weight polymers. Poly(acrylic acid) microgel beads show also a size exclusion upon binding of oppositely charged polyelectrolytes.[36,67] These beads with sizes of 80−100 μm can be used for binding and release of e.g. peptides.[68]

The *ccns* microgel investigated in our study combines both porosity and compartmentalization on a nanometer length scale. Binding of high-MW polyelectrolyte on the surface leads to charge reversal while low-MW polyelectrolyte can be encapsulated in the core and protected by the shell. Thus, complexes of core−shell microgels and polyelectrolyte can be used as stimuli-sensitive nanocontainers.

The polyelectrolyte's possibility to penetrate through a neutral shell into the charged core of a microgel was also observed in the fluorescence study involving labeled PLL as polycation. The experimental observation that the PLL^{FITC} shows the same lifetime for the *cc* and *ccns* microgels (but a different lifetime as compared to the complexes with the *nccs* microgel; see Figure 8) indicates that the polyelectrolyte is in the same environment for both the *cc* and *ccns* microgels. This strongly indicates that the PLL is located in the charged core for these two microgels. For the core−shell microgel *ccns* this requires a penetration of the PLL through the uncharged shell to the negative charges located in the core. These results are thus in very good agreement with studies on the PDADMAC−microgel systems, which also indicated that the polyelectrolyte is able to penetrate through the neutral shell into the charged core.

The results demonstrate that charged microgels can *ab*sorb and *ad*sorb polyelectrolytes of opposite charge. The degree of penetration depends on the chain length of the polyelectrolyte as well as on the microgel architecture.

Summary. Three charged microgels (namely charged core, *cc*; charged core−neutral shell, *ccns*; neutral core−charged shell, *nccs*) were prepared by sequential synthesis. The spatial distribution of the charged monomers inside the microgel is different. The methacrylic acid functions were either exposed at the surface (neutral core−charged shell) or located inside the particle (charged core−neutral shell).

Two batches of polyelectrolyte differing in the molecular weight were employed and the amount of polyelectrolyte bound to the different microgels was quantified. The spatial distribution of charges inside the microgel determines the amount of bound polyelectrolyte and the electrophoretic mobility of the complex. High-MW polyelectrolyte adsorbs close to the surface of the microgel (or the shell) while the low-MW polyelectrolyte can penetrate through a shell into the microgel core as demonstrated by composition, electrophoretic mobility, and lifetime of fluorescence label.

Furthermore, almost equal *icr*/*ncr* plots for *cc* and *ccns* microgels indicate that the interaction of PNiPAM-*co*-MAA microgels and PDADMAC is mainly driven by electrostatics. Normalization of the bound polyelectrolyte mass to the charges of the microgels shows that both *cc* and *ccns* microgels have the same ability to bind PDADMAC.

The results demonstrate the microgels are able to absorb or adsorb polyelectrolytes depending on the polyelectrolyte's chain length and the microgels architecture. Thus, microgels offer properties that are distinctly different from rigid nanoparticles. Complexes with different surface properties and different colloidal stability can be prepared easily. In addition, polyelectrolytes can be encapsulated in the microgel core and protected by the shell. Thus, multisensitive core−shell microgels combine permeability and compartmentalization on a nanometer length scale. As the shell is penetrable by polymers, such microgels provide unique opportunities for applications e.g. in controlled uptake and release.

Acknowledgment. We thank Michael Kather for help with the microgel synthesis and complex formation. Dr. Hamann (Katpol, Germany) is thanked for providing PDADMAC. This work was supported by the Deutsche Forschungsgemeinschaft.

Supporting Information Available: Radii of the complexes were measured as a function of the bound amount of PDADMAC (*ncr*); temperature-dependent size measurements of complexes prepared from the *ccns* and the *nccs* microgels with low-MW PDADMAC. This material is available free of charge via the Internet at http://pubs.acs.org.

(61) Wagberg, L.; Hägglund, R. *Langmuir* **2001**, *17*, 1096–1103.
(62) Horvath, A. E.; Lindström, T.; Laine, J. *Langmuir* **2006**, *22*, 824–830.
(63) Malinova, V.; Wandrey, C. *J. Phys. Chem. B* **2007**, *111*, 8494–8501.
(64) Mishael, Y. G.; Dubin, P. L.; de Vries, R.; Baska Kayitmazer, A. *Langmuir* **2007**, *23*, 2510–2516.
(65) Schmidt, B.; Wandrey, C.; Freitag, R. *J. Chromatogr., A* **2002**, *944*, 149–159.
(66) Schmidt, B.; Wandrey, C.; Freitag, R. *J. Chromatogr., A* **2003**, *1018*, 155–167.
(67) Bysell, H.; Hansson, P.; Malmsten, M. *J. Colloid Interface Sci.* **2008**, *323*, 60–69.
(68) Bysell, H.; Schmidtchen, A.; Malmsten, M. *Biomacromolecules* **2009**, *10*, 2162–2168.